Chapter 14
A Joint Energy Storage Systems and Wind Farms Long-Term Planning Model Considering Voltage Stability

Saman Nikkhah and Abbas Rabiee

14.1 Introduction

Radially nature and high ratio of R/X in distribution systems (DSs) cause several operational and security problems such as high power losses and low voltage profile in the grid. Recently, several solutions have been suggested to improve the reliability and stability of DSs. In spite of their costs, distributed generations (DGs) are considered to be one of the best viable solutions for these problems. Undeniable advantages of wind energy in today's power systems have resulted in rapid increase in penetration level of this kind of renewable energy sources into local and regional utility grids. However, despite various advantages of wind power technology, intermittent and stochastic nature of such DG resource can cause noticeable challenges for distribution system operators (DSOs), especially from the voltage stability point of view.

Recently, the integration of wind energy in DSs with energy storage systems (ESSs) has become a new solution to ensure the stability and reliability of a power system with facilitating increased penetration of wind energy. The dispatchable storage technologies can also provide additional benefits for distribution utilities, including better load management [1], mitigating power quality concerns [2], and overall reduction of energy costs [3]. In the following subsection, a review is made on previous researches in this regard and a background is made on planning of ESS to solve the uncertainty problem of renewable energy sources.

S. Nikkhah · A. Rabiee (✉)
Faculty of Electrical Engineering, University of Zanjan, Zanjan, Iran
e-mail: s.nikkhah@znu.ac.ir; rabiee@znu.ac.ir

B. Mohammadi-Ivatloo, F. Jabari (eds.), *Operation, Planning, and Analysis of Energy Storage Systems in Smart Energy Hubs*,
https://doi.org/10.1007/978-3-319-75097-2_14

14.1.1 Review of the Existing Literature

The ESS planning in DSs has been addressed in several research works. In [4], the authors propose a stochastic planning framework for storage systems to optimally site the battery ESS, aiming to maximize wind power penetration and minimize operation and investment costs. The uncertainty of wind energy is modeled by Monte Carlo simulations. In [5], a methodology is proposed for optimal allocation of ESS for a system with high penetration of wind energy. Both perspectives of the utility and the DG owner are taken into consideration by sizing the ESS to accommodate all amount of spilled wind energy. The authors of [6] consider a tradeoff between budget for investment and the daily operation cost in the ESS planning. The information gap decision theory is used in [7] for handling wind power uncertainty. The authors investigate the effect of storage devices on the uncertainty handling of wind energy. In [8], a multi-objective optimization model is proposed for scheduling of ESSs. In [9], the system robust operation ensured by using robust optimization technique, while the investment costs of storage units are minimized. The authors in [10] focus on the loss payment minimization using ESS and demand response in an uncertain environment, while electricity price is considered as an uncertain parameter. The work in [11] suggests a comprehensive framework for ESS allocation, aiming to increase wind power penetration and voltage stability enhancement. The authors consider economic requirements such as cost and profit obtained by sizing and siting of the ESSs.

Different objectives are addressed in the existing literature for the ESS scheduling problem. The economic objective in [12] is minimization of electricity usage cost and battery operation costs. In [13], a stochastic planning framework is proposed from the perspective of independent system operator aiming to maximize several objectives including: total expected net present value (NPV), cost and benefit of electricity utilization, power generation, etc. In [14], an economic dispatch model is proposed to increase wind utilization by utilization of ESSs with the objective of minimizing the composite operating costs of the system. The authors in [15] consider a coordinated wind power and ESS model for decreasing wind energy forecast errors. In [16], a probabilistic optimal power flow is introduced for optimal placement of ESSs in a system with the objective of minimizing the hourly social cost. In [17], the impact of ESS specific costs on the NPV of ESS installation investment is investigated considering the relationship between wind power penetration and daily load profile. In [18], the size of ESS installed in a wind-diesel power system is determined via a two-stage stochastic optimization model, with the objectives of fuel cost and operating cost minimization.

Although voltage stability is considered in some wind power planning research works [19–21], and improvement of voltage stability with application of ESS has been investigated in the literatures [22–26], the point which is not considered in previous works is consideration of voltage stability as a constraint of joint ESS and wind energy planning models. In [19], system loading margin (LM) is considered as

constraints in the proposed corrective voltage control scheme for a system under the influence of wind energy. The work in [20] proposes voltage stability constrained optimal power flow which the relationship between the LM and uncertainty of wind energy is investigated. In [21], the improvement of voltage stability of power system under the influence of wind power generation is investigated while L-index considered as the voltage stability index. The work in [22], proposes a combinational photovoltaic and ESS model to improve voltage stability and decrease active and reactive power losses by optimal dispatching of load power factor. The customer-side ESSs are used in [23] to solve the voltage fluctuations of DSs with high penetration of photovoltaic systems, by giving the permission to DSO to control the output of ESSs. In [24], a coordinated control approach is proposed for decreasing the voltage and frequency deviations. Also, in [24] the voltage profile of a real DS is improved by coordinated operation of ESS and photovoltaic system. Due to the potential of battery ESS and STATCOM, the work in [25] is focused on the improvement of power quality and stability of DSs under the influence of high wind power penetration. In [26], grid voltage stability is improved while acceptable wind power penetration obtained by using ESS to control the intermittent nature of wind energy.

While the aim of the proposed models in the existing literature is improving voltage stability, this chapter considers the voltage stability as a constraint in the proposed model and optimal capacity of ESSs and wind turbines (as a kind of DGs) obtained subject to secure operation of power system from voltage stability point of view.

14.1.2 Chapter Contributions

It is concluded from the above literature survey that various planning frameworks have been proposed in the area of sizing and scheduling of ESS to mitigate the problems associated with the uncertainty of renewable DG units, and optimizing several objectives. However, the voltage stability considerations have not been included in the formulation of proposed models. Furthermore, the concept of integrating ESS in the system under the influence of wind energy from the perspectives of both DG owners and DSO has not been considered simultaneously. Therefore, the main focus of this chapter is to propose a voltage stability constrained wind-storage planning model (VSC-WSPM) which considers the perspectives of both DG owner and DSO. Due to the fact that one of the system operator's goals is minimizing power generation costs while preserving the system stability [27], the objective of the proposed model is to minimize power generation costs and charge/discharge costs of ESSs and to maximize the profit obtained by DG owner from wind energy procurement.

The main contributions of this chapter are outlined as follows:

- A comprehensive model is proposed for simultaneous planning of wind energy and ESS.
- The welfare of both DSO and DG owners is considered simultaneously in the long-term planning horizon.
- Voltage stability considered in the planning model.
- The impact of voltage stability on the capacity of DGs and ESSs is investigated.
- Optimal capacity of ESSs and DGs is determined in the entire planning horizon.

14.2 The Concept of Loading Margin Index for Voltage Stability Evaluation

LM is defined as the amount of power generation that can be increased to meet the additional demand increase in PQ buses prior to violation of operational limits or happening voltage collapse [28]. In order to guarantee the secure operation of a power system, it is necessary to preserve a desired level of LM. This level of LM specifies the distance between normal operation point and voltage collapse point of the system [29]. In this regard, power flow equations at the current operation point (COP) considered along with power flow equations in loadability limit point (LLP) (e.g., the nose point of PV curve), simultaneously [20].

For better description of the LM concept, consider the PV curve of an arbitrary load bus of a system that is depicted in Fig. 14.1. The points A and B are the system COP and the corresponding LLP, respectively. The distance (in MW or MVA) between points A and B is called LM, which could be characterized by loading parameter, λ. In order to have a proper safety margin, the system operator considers a desired level for the LM in which the system LM should be greater than it. The amount of system LM is an important factor for secure operation of the system, since the voltage instability can be prevented in the post-contingency conditions, if a sufficient LM is considered.

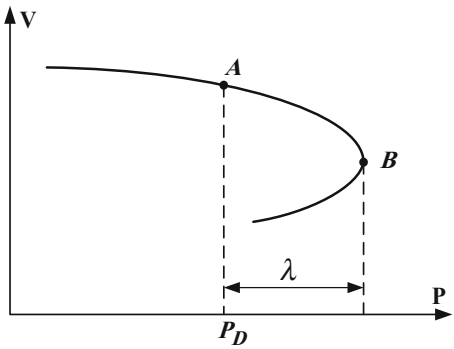

Fig. 14.1 System loading margin of P-V curve [20]

The generator's reactive power support is one of the most important factors which directly influences the system LM. The system LM will be large, when enough reactive power support exists in the system. Consequently, insufficient reactive power support or reaching the reactive power limit of generators could cause voltage collapse.

In this chapter, the LM is included in VSC-WSPM and power flow equality and inequality constraints considered in both LLP and COP points, simultaneously, in order to characterize the LM.

14.3 VSC-WSPM Problem Formulation

14.3.1 Objective Functions

The objective function of the problem is optimized by considering the minimization of power generation and ESS operation costs and maximization of wind energy profit obtained by DG owners.

14.3.1.1 Minimization of Power Generation Costs

Minimizing the total power generation cost in DSs is critical objective and should be considered in long-term planning models for improving total energy efficiency and economic reasons.

$$F_1 = \sum_{n=1}^{N_T} \sum_{t=1}^{24} 365 \times \left(\frac{1+\vartheta}{1+\varepsilon} \right)^n \cdot \mathrm{EC}_{n,t} \times \left(\sum_{i=1}^{N_G} P_{i,n,t}^{G} + \sum_{b=1}^{N_{\mathrm{DG}}} p_{b,n,t}^{\mathrm{DG}} \right) \tag{14.1}$$

where F_1 is the total power generation cost in planning horizon, $P_{i,n,t}^{G}$ and $p_{b,n,t}^{\mathrm{DG}}$ are active power generation and injected wind power to the grid at bus b in year n and time t, respectively. Also, $\mathrm{EC}_{n,t}$ is the energy cost in year n and time t, ϑ and ε are inflation and interest rates, respectively.

14.3.1.2 Minimization of ESS Charge/Discharge Costs

The ESS charge/discharge cost is a critical operation objective that should be minimized during the planning horizon.

$$F_2 = \sum_{n=1}^{N_T} \sum_{t=1}^{24} \sum_{b=1}^{N_{\mathrm{ESS}}} 365 \times \left(\frac{1+\vartheta}{1+\varepsilon} \right)^n \times \mathrm{CHC}_{n,t} \times \Delta t \left(p_{b,n,t}^{\mathrm{CH}} \cdot \eta_{b,t}^{\mathrm{ch}} + p_{b,n,t}^{\mathrm{DISCH}} / \eta_{b,t}^{\mathrm{disch}} \right) \tag{14.2}$$

where F_2 is the total ESS charge/discharge cost in planning horizon, $p_{b,n,t}^{\mathrm{CH}}/p_{b,n,t}^{\mathrm{DISCH}}$ are charge/discharge power of ESS at node b in year n and time t, $\eta_{b,t}^{\mathrm{ch}}/\eta_{b,t}^{\mathrm{disch}}$ are charging/discharging efficiencies, $\mathrm{CHC}_{n,\,t}$ is the operation cost of ESS.

14.3.1.3 Maximization of the Profit Obtained from the Wind Energy Procurement

The objective of DG owners is to maximize the net present value (NPV) of profit based on the annual cash flow over the time horizon of the investment.

$$F_3 = \left(\frac{1+\vartheta}{1+\varepsilon}\right)^n \times \left(\sum_{t=1}^{24}\sum_{n=1}^{N_T}\sum_{b=1}^{N_W}\left(\mathrm{IN}_{b,n,t}^{\mathrm{inc}} - C_{b,n,t}^{\mathrm{O\&M}}\right) - \sum_{n=1}^{N_T}\sum_{b=1}^{N_W} C_{b,n}^{\mathrm{inv}}\right) \tag{14.3}$$

where $\mathrm{IN}_{t,d,b}^{\mathrm{inc}}$ is the total annualized incoming of wind energy selling to the costumers and $C_{t,d,b}^{\mathrm{O\&M}}$ corresponds to the operation and maintenance cost of DGs, whereas $C_{t,b}^{\mathrm{inv}}$ denotes the DGs investment cost. These costs are formulated as follows:

$$\mathrm{IN}_{b,n,t}^{\mathrm{inc}} = p_{b,n,t}^{\mathrm{DG}} \times \mathrm{EC}_{n,t} \tag{14.4}$$

$$C_{b,n,t}^{\mathrm{O\&M}} = p_{b,n,t}^{\mathrm{DG}} \times \mathrm{DGC}_{\mathrm{O\&M}} \tag{14.5}$$

$$C_{b,n}^{\mathrm{inv}} = P_{b,n}^{\mathrm{DG}} \times \mathrm{DGC}_{\mathrm{inv}} \tag{14.6}$$

where $P_{b,n}^{\mathrm{DG}}$ is the added wind energy capacity to the grid at bus b in year n, $\mathrm{DGC}_{\mathrm{O\ \&\ M}}$ and $\mathrm{DGC}_{\mathrm{inv}}$ are operation and maintenance cost ($/MWh) and investment cost ($/MW) of DGs, respectively.

14.3.2 The Overall Objective Function

In order to consider all mentioned objective functions in one objective, two coefficients defined as the weighting coefficients which basically amounted in the interval [0, 1]. These coefficients are called w_1 and w_2. Due to this explanation, the total objective function which is the minimization of social welfare is defined as follows:

$$\mathrm{OF} = \min\left(w_1 \times (F_1 + F_2) - w_2 \times F_3\right) \tag{14.7}$$

14.3.3 Constraints

The VSC-WSPM is subject to following operation constraints.

14.3.3.1 Power Balance Constraints at COP

In order to optimize the objective function of proposed VSC-WSPM, it is necessary to consider the power flow constrains, operational and physical limits. Due to consideration of LM as the voltage stability index, the equality and inequality constraints at LLP should be considered additionally. In the following, a detailed description of equality and inequality constrains at COP are given.

$$\begin{aligned}\left(\sum_{i=1}^{N_G} P_{i,n,t}^{G}\right) + p_{b,n,t}^{\mathrm{DG}} + p_{b,n,t}^{\mathrm{DISCH}} - P_{b,n,t}^{D} - p_{b,n,t}^{\mathrm{CH}} \\ = V_{b,n,t} \sum_{j=1}^{N_B} V_{j,n,t} Y_{bj} \cos\left(\theta_{b,n,t} - \theta_{j,n,t} - \phi_{bj}\right)\end{aligned} \tag{14.8}$$

$$\left(\sum_{i=1}^{N_G} Q_{i,n,t}^{G}\right) + q_{b,n,t}^{\mathrm{DG}} - Q_{b,n,t}^{D} = V_{b,n,t} \sum_{j=1}^{N_B} V_{j,n,t} Y_{bj} \sin\left(\theta_{b,n,t} - \theta_{j,n,t} - \phi_{bj}\right) \tag{14.9}$$

$$P_{G_i}^{\min} \le P_{i,n,t}^{G} \le P_{G_i}^{\max} \tag{14.10}$$

$$Q_{G_i}^{\min} \le Q_{i,n,t}^{G} \le Q_{G_i}^{\max} \tag{14.11}$$

$$V_b^{\min} \le V_{b,n,t} \le V_b^{\max} \tag{14.12}$$

$$|S_{l,n,t}(V, \theta)| \le S_l^{\max} \tag{14.13}$$

where constraints (14.8) and (14.9) are the power flow equations at COP, $P_{i,n,t}^{G}$, $Q_{i,n,t}^{G}$ are active and reactive power production of generator at bus i, in year n and time t, $P_{b,n,t}^{D}$, $Q_{b,n,t}^{D}$ are active and reactive power demand of b-th bus in year n and time t, Y_{bj}, ϕ_{bj} magnitude/angle of bj-th element of system admittance matrix, $V_{b,\,t,\,d}/\theta_{b,\,t,\,d}$ voltage magnitude/angle of bus b in year n and time t. Also, constraints (14.10)–(14.12) show the active and reactive power of the generators and voltage of system buses, respectively. Also, (14.13) shows the limit on power flowing through the branches.

14.3.3.2 Power Balance Constraints at LLP

As it is aforementioned, in the proposed VSC-WSPM, it is necessary to consider operational constraints at LLP in addition to considering those of COP. The following constraints represent the proposed constraints that considered in LLP.

$$\left(\sum_{i=1}^{N_G} \widehat{P}^{G}_{i,n,t}\right) + p^{\mathrm{DG}}_{b,n,t} + p^{\mathrm{DISCH}}_{b,n,t} - \widehat{P}^{D}_{b,n,t} - p^{\mathrm{CH}}_{b,n,t} = \widehat{V}_{b,n,t} \sum_{j=1}^{N_B} \widehat{V}_{j,n,t} Y_{bj} \cos\left(\widehat{\theta}_{b,n,t} - \widehat{\theta}_{j,n,t} - \phi_{bj}\right) \tag{14.14}$$

$$\left(\sum_{i=1}^{N_G} \widehat{Q}^{G}_{i,n,t}\right) + q^{\mathrm{DG}}_{b,n,t} - \widehat{Q}^{D}_{b,n,t} = \widehat{V}_{b,n,t} \sum_{j=1}^{N_B} \widehat{V}_{j,n,t} Y_{bj} \sin\left(\widehat{\theta}_{b,n,t} - \widehat{\theta}_{j,n,t} - \phi_{bj}\right) \tag{14.15}$$

$$\widehat{P}^{D}_{b,n,t} = (1 + K_{D,b}\lambda)\, P^{D}_{b,n,t} \tag{14.16}$$

$$\widehat{Q}^{D}_{b,n,t} = (1 + K_{D,b}\lambda)\left(Q^{D}_{b,n,t}\right) \tag{14.17}$$

$$\widehat{P}^{G}_{i,n,t} = \min\left(P^{\max}_{G_i}, (1 + K_{G,i}\lambda)\, P^{G}_{i,n,t}\right) \tag{14.18}$$

$$P^{\min}_{G_i} \le \widehat{P}^{G}_{i,n,t} \le P^{\max}_{G_i} \tag{14.19}$$

$$Q^{\min}_{G_i} \le \widehat{Q}^{G}_{i,n,t} \le Q^{\min}_{G_i} \tag{14.20}$$

$$V^{\min}_{b} \le \widehat{V}_{b,n,t} \le V^{\max}_{b} \tag{14.21}$$

$$\left|\widehat{S}_{l,n,t}(V, \theta)\right| \le S^{\max}_{l} \tag{14.22}$$

$$\lambda \ge \lambda_{\mathrm{des}} > 0 \tag{14.23}$$

where (14.14) and (14.15) show the power flow equations at LLP, (14.16) and (14.17) correspond to the active and reactive power increment pattern of loads to meet the load increased from COP to LLP. $\widehat{P}^{G}_{i,n,t}$, $\widehat{Q}^{G}_{i,n,t}$ are active and reactive power production of generator at bus i, in year n and time t, at LLP, $\widehat{P}^{D}_{b,n,t}$, $\widehat{Q}^{D}_{b,n,t}$ are active and reactive power consumption of load connected to b-th bus in year n and

time t, at LLP, $\widehat{V}_{j,\mathrm{n,t}}/\widehat{\theta}_{b,\mathrm{n,t}}$ is voltage magnitude/angle of bus b in year n and time t, at LLP. Also, (14.18) shows the increment of generators active power to cover the demand increment from the COP to the LLP. Also, constraints (14.19)–(14.22) correspond to active/reactive power limits, voltage magnitude limits, and the limits of apparent power flowing through branches at LLP, respectively. Finally, as it is aforementioned, desired value of LM that is defined by DSO should be lower than loading parameter, which is considered in (14.23).

14.3.3.3 System Load Growth

This chapter deals with the planning of ESSs and DGs in long-term planning horizon. Therefore, it is necessary to consider daily load model which considers the annual demand growth. This concept is mathematically expressed as follows:

$$P^{D}_{b,n,t} = (1 + \beta_{b,n})\, P^{D}_{b,n-1,t} \tag{14.24}$$

$$Q^{D}_{b,n,t} = (1 + \beta_{b,n})\, Q^{D}_{b,n-1,t} \tag{14.25}$$

where $\beta_{b,\,n}$ is the annually load growth for system load buses.

14.3.3.4 DG Capacity Constraints

Intermittency of wind energy is one of the main barriers against the high penetration of wind power in a grid. Therefore, it is necessary to limit the active and reactive capacity of each DG as follows:

$$0 \le \sum_{b} \pi^{\mathrm{DG}}_{b,n} \le \rho \times \sum_{b} P^{D}_{b,n,t} \tag{14.26}$$

$$\pi^{\mathrm{DG}}_{b,n} = \pi^{\mathrm{DG}}_{b,n-1} + P^{\mathrm{DG}}_{b,n} \tag{14.27}$$

$$P^{\mathrm{DG}}_{b,n} \le I^{\mathrm{DG}}_{b,n} \cdot P^{\mathrm{DG}}_{\min},\ \left(I^{\mathrm{DG}}_{b,n} \in \{0,1\}\right) \tag{14.28}$$

$$P^{\mathrm{DG}}_{b,n} \ge I^{\mathrm{DG}}_{b,n} \times P^{\mathrm{DG}}_{\max} \tag{14.29}$$

$$0 \le p^{\mathrm{DG}}_{b,n,t} \le \mathrm{CF}^{\mathrm{DG}}_{t} \times \pi^{\mathrm{DG}}_{b,n} \tag{14.30}$$

$$q^{\mathrm{DG}}_{b,\min} \le q^{\mathrm{DG}}_{b,n,t} \le q^{\mathrm{DG}}_{b,\max} \tag{14.31}$$

where (14.26) gives the cumulative wind energy limit in n-th year of the planning horizon, which is increased in each year over the previous year due to the added wind capacity to the grid as shown in (14.27). Due to the economic and operational limits, added wind energy to the grid should be limited by (14.28) and (14.29) which binary variable $I_{b,n}^{\mathrm{DG}}$ denotes the years that wind energy needed to be added to the grid for a DG connected to bus b. Whereas, the DGs actual power output that is used in (14.8) and (14.9) is limited by (14.30) due to the capacity factor (CF) of DGs. Besides, (14.31) denotes the reactive power generation limits of the DGs.

14.3.3.5 ESS Constraints

The ESSs have technical operation constraints and should be considered in planning model. The ESS constraints proposed in this chapter are expressed as follows:

(a) Charging/discharging power constraints

$$0 \le p_{b,n,t}^{\mathrm{CH}} \le \delta_{b,t}^{\mathrm{ch}} \times p_{b,t}^{\mathrm{ch,max}} \tag{14.32}$$

$$0 \le p_{b,n,t}^{\mathrm{DISCH}} \le \delta_{b,t}^{\mathrm{disch}} \times p_{b,t}^{\mathrm{disch,max}} \tag{14.33}$$

$$\sum_{b}^{N_{\mathrm{ESS}}} \sum_{t=1}^{24} p_{b,n,t}^{\mathrm{CH}} \ge \sum_{b}^{N_{\mathrm{ESS}}} \sum_{t=1}^{24} p_{b,n,t}^{\mathrm{DISCH}} \tag{14.34}$$

$$\delta_{b,t}^{\mathrm{ch}} + \delta_{b,t}^{\mathrm{disch}} \le 1, \left(\delta_{b,t}^{\mathrm{disch}}, \delta_{b,t}^{\mathrm{ch}} \in \{0, 1\}\right) \tag{14.35}$$

where (14.32) and (14.33) show the charging/discharging power limit. Also, due to the operation schedule of ESS, charging capacity of storage should be greater than discharging capacity of storage, which is modeled in (14.34). Also, (14.35) denotes that in each time interval t, only charge or discharge of ESSs is allowed.

(b) State of charge constraints

$$\mathrm{SOC}_{b}^{\mathrm{min}} \le \mathrm{SOC}_{b,n,t}^{\mathrm{ESS}} \le \mathrm{SOC}_{b}^{\mathrm{max}} \tag{14.36}$$

$$\mathrm{SOC}_{b,n,t}^{\mathrm{ESS}} \le E_{b,n-1}^{\mathrm{ESS}} \tag{14.37}$$

$$E_{b,n+1}^{\mathrm{ESS}} = E_{b,n}^{\mathrm{ESS}} + e_{b,n}^{\mathrm{ESS}} \tag{14.38}$$

$$0 \leq e_{b,n}^{\mathrm{ESS}} \leq e_{\max}^{\mathrm{ESS}} \tag{14.39}$$

$$\mathrm{SOC}_{b,n+1,t}^{\mathrm{ESS}} = \mathrm{SOC}_{b,n,t}^{\mathrm{ESS}} + \Delta t \times \left(p_{b,n,t}^{\mathrm{CH}} \eta_{b,t}^{\mathrm{ch}} - p_{b,n,t}^{\mathrm{DISCH}} / \eta_{b,t}^{\mathrm{disch}}\right) \tag{14.40}$$

where constraint (14.36) shows the allowable state of charge of storage. Also according to (14.37) $\mathrm{SOC}_{b,n,t}^{\mathrm{ESS}}$ is the state of charge (SOC) for ESS installed at bus b, in year n and time t which is lower than total capacity of ESS installed till the n-th year ($E_{b,n-1}^{\mathrm{ESS}}$). The total capacity of ESSs increased each year over the previous year due to the added capacity of ESSs ($e_{b,n}^{\mathrm{ESS}}$) in each year which is shown by (14.38). Also, the annual capacity expansion of ESSs is limited by (14.39). Furthermore, the relationship between charging/discharging power and SOC of ESSs is modeled in (14.40), where Δt is the time slot of daily schedule which is assumed to be 1 h.

14.4 Simulations on a Standard Test System

In this section, the proposed VSC-WSPM is examined on a standard test system. In order to show the different aspects of the proposed model, different cases are considered. The following subsection gives the system data and the model parameters.

14.4.1 System Description

In order to evaluate the performance of the proposed VSC-WSPM, simulations are performed on the IEEE 33-bus standard distribution feeder. This system consists of 33 buses and 32 branches. The single line diagram of this system is depicted in Fig. 14.2. The proposed VSC-WSPM model, which is a mixed integer nonlinear programming problem (MINLP), is implemented in General Algebraic Modeling System (GAMS) [30] using DICOPT [31] and IPOPT [32] solvers. It is assumed that the demand of load buses varies in 24 h of a day with a pattern given in Fig. 14.3, while it is increased by 2% per year in the next years. It is assumed that three DGs are installed at buses 6, 14, and 32 whereas the penetration level (ρ) of DGs is supposed to be 50%. A planning horizon of 5 years is considered. It is assumed that DG units' yearly added capacity limited within 1–2 MW. Also, it is assumed that there is no injected wind energy to the grid during the first year to cope with budgeting delays and possible changes in policies. The proposed VSC-WSPM has been solved using parameters of Table 14.1. Table 14.2 summarizes the characteristics of dispatchable DG units. Also, Table 14.3 provides the daily variation of DGs' CF.

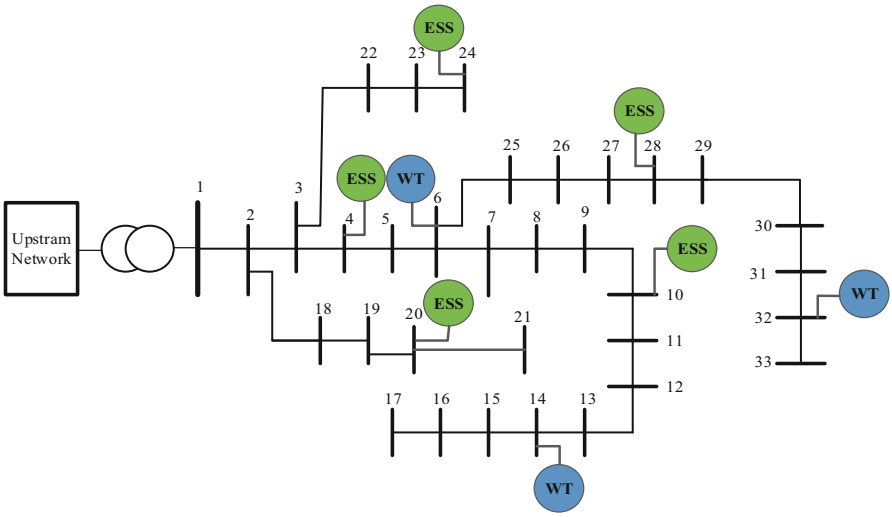

Fig. 14.2 Single line diagram of IEEE 33-bus distribution feeder

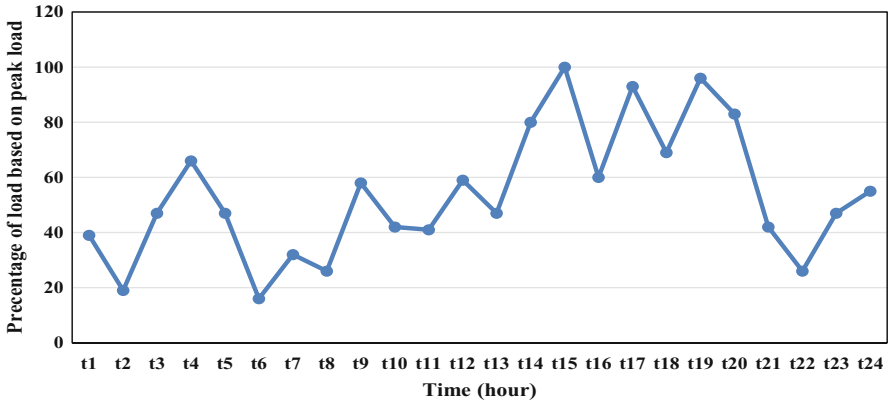

Fig. 14.3 Variation of load at load buses for 24 h of a day based on the peak value

Table 14.1 The simulation parameters

Parameter	Values (%)
$\beta_{b,t}$	2
ρ	50
λ_{des}	5
ITR	6
IFR	1

Table 14.2 Characteristics of dispatchable DG units [33]

Parameter	Unit	Value
DGs investment cost	\$/MW	318,000
DGs operation and maintenance cost	\$/MWh	10

Table 14.3 Daily variation of $\mathbf{CF}_t^W$

t_1	t_2	t_3	t_4	t_5	t_6	t_7	t_8	t_9	t_{10}	t_{11}	t_{12}
0.84	0.73	0.51	0.14	0.48	0.47	0.87	0.86	0.32	0.82	0.55	0.75
t_{13}	t_{14}	t_{15}	t_{16}	t_{17}	t_{18}	t_{19}	t_{20}	t_{21}	t_{22}	t_{23}	t_{24}
0.26	0.96	0.31	0.34	0.44	0.43	0.16	0.42	0.8	0.29	0.82	0.36

Table 14.4 Characteristics of ESS

$p_{b,t}^{\text{ch,max}}$ (MW)	$p_{b,t}^{\text{disch,max}}$ (MW)	$\eta_{b,t}^{\text{ch}}$	$\eta_{b,t}^{\text{disch}}$	$e_{\max}^{\text{ESS}}$ (MWh)
1	1	0.88	0.88	7

Table 14.5 Energy price ($\text{EC}_{n,t}$(\$/MWh))

t_1	t_2	t_3	t_4	t_5	t_6	t_7	t_8	t_9	t_{10}	t_{11}	t_{12}	t_{13}	t_{14}	t_{15}	t_{16}	t_{17}	t_{18}	t_{19}	t_{20}	t_{21}	t_{22}	t_{23}	t_{24}
40	36	48	54	48	36	38	36	52	44	42	52	47	60	60	52	60	57	60	60	44	36	48	50

Table 14.6 Charge/discharge cost of ESS ($\text{CHC}_{n,t}$(\$/MWh))

t_1	t_2	t_3	t_4	t_5	t_6	t_7	t_8	t_9	t_{10}	t_{11}	t_{12}	t_{13}	t_{14}	t_{15}	t_{16}	t_{17}	t_{18}	t_{19}	t_{20}	t_{21}	t_{22}	t_{23}	t_{24}
7	6	8	9	8	6	7	6	9	7	7	9	7.8	10	10	9	10	10	10	10	7	6	8	8

The buses 4, 10, 20, 24, and 28 selected for installation of ESSs. It is assumed that the ESSs will not charge or discharge in the first year of planning. Also, it is assumed that the SOC of each year equals to the amount of SOC at the end of previous year and the final energy stored in the ESSs at the end of a day, considered to be the initial state of ESSs in the next day. It is worth mentioning that each day simply models the peak load condition of a year, and since it is assumed the 5 years planning horizon, the 5 consecutive days considered accordingly. Characteristics of ESS, energy price, and charging cost of ESS are tabulated in Tables 14.4, 14.5, and 14.6, respectively.

In the following, the results obtained by implementing the proposed VSC-WSPM on IEEE-33 bus distribution test system are presented. The problem is examined in three case studies namely: Case-I: from the perspective of DSO (i.e., $w_1 = 1$, $w_2 = 0$, in Eq. (14.7)), Case-II: from the perspective of DG owner (i.e., $w_1 = 0$, $w_2 = 1$, in Eq. (14.7)), Case-III: from the perspective of both DG owner and DSO, simultaneously (i.e., $w_1 = w_2 = 0.5$, in Eq. (14.7)). In these cases, in order to show the effect of voltage stability constraints on the scheduled capacity of DGs and ESSs, Cases I and II solved with and without voltage stability constraints (i.e., without Eqs. (14.14)–(14.23)). For the sake of comparison, the results obtained for different cases are compared in Case-III.

14.4.2 Case-I: From the Perspective of DSO

In this case the proposed VSC-WSPM is implemented with and without the voltage stability constraints, from the perspective of DSO. Power generation cost with and without voltage stability constraints in this case is \$4103451.9 and \$4112595.9, respectively. Therefore, including voltage stability constraints imposes more cost to the DSO, which is reasonable. The annual added capacity of ESSs and DGs in this case for the entire planning horizon is depicted in Figs. 14.4 and 14.5, respectively. As it is observed from these figures, when voltage stability constraints

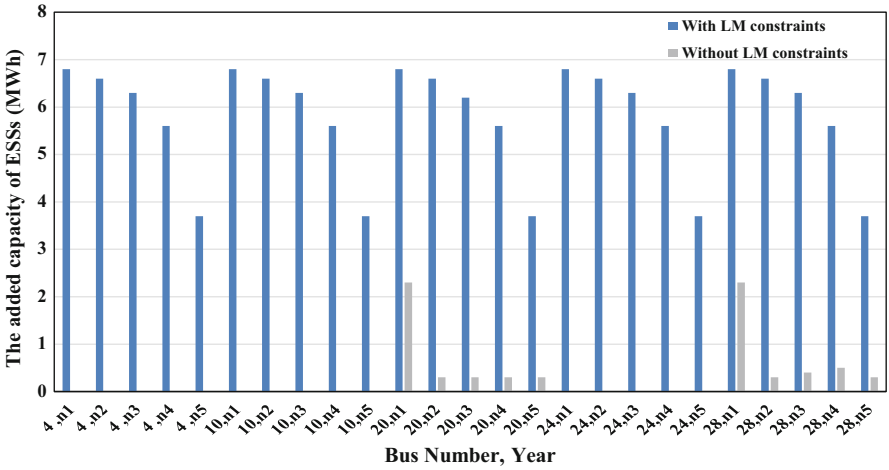

Fig. 14.4 The added capacity of ESSs in each bus number for planning horizon, in Case-I

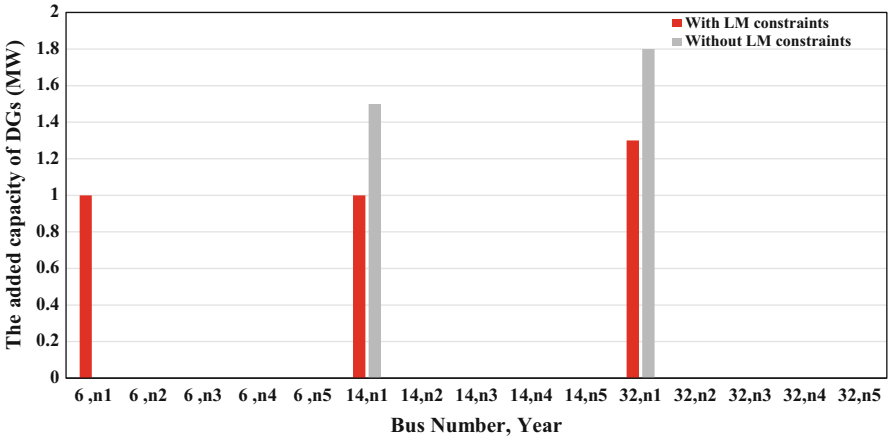

Fig. 14.5 The added capacity of DGs in each bus number for planning horizon in Case-I

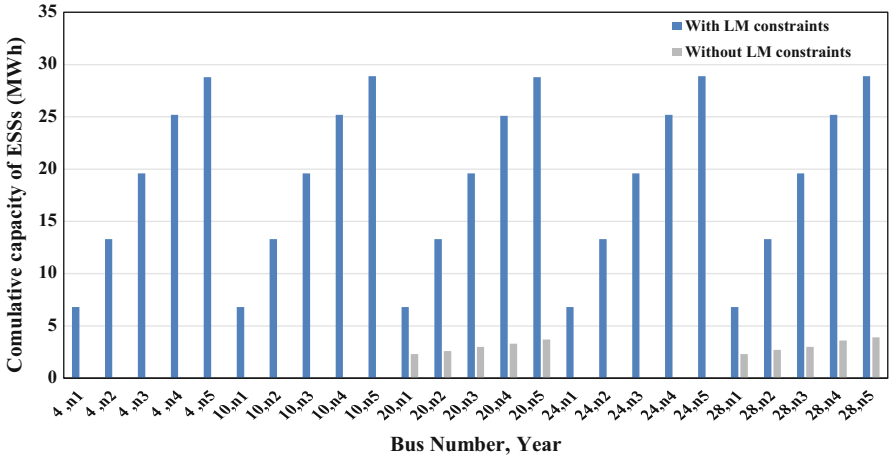

Fig. 14.6 Total capacity of ESSs in each bus for the planning horizon in Case-I

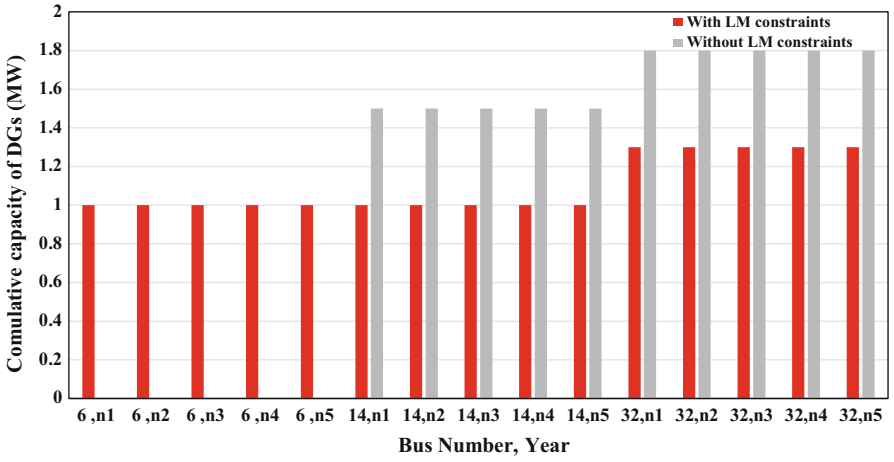

Fig. 14.7 Total capacity of DGs in each bus number for planning horizon, in Case-I

are considered in the VSC-WSPM, more wind power and ESS power are added to the grid in order to prevent voltage instability.

Besides, the total installed capacity of ESSs and DGs are depicted in Figs. 14.6 and 14.7, respectively. As it is observed from these figures, total capacities of wind energy and ESSs are affected by voltage stability constraints. It is evident from Fig. 14.6 that total capacity of ESSs increases yearly because additional capacity is added to the grid in each year. Also, for the DGs, no new capacity is scheduled since first year and total capacity is fixed in planning horizon for each installed DG bus number.

14.4.3 Case-II: From the Perspective of DG Owner

In this section the problem is solved from the DG owner's perspective and the effect of voltage stability constraints on the capacity of DGs and ESSs investigated. The net profit obtained from sharing wind energy with and without voltage stability constraints in this case is \$875527.7 and \$897296.7, respectively. It is worth to note that considering voltage stability decreases the DG owner's profit. The annual added capacity of ESSs and DGs in this case for the entire planning horizon is given in Figs. 14.8 and 14.9, respectively. It is inferred from these figures that adding wind

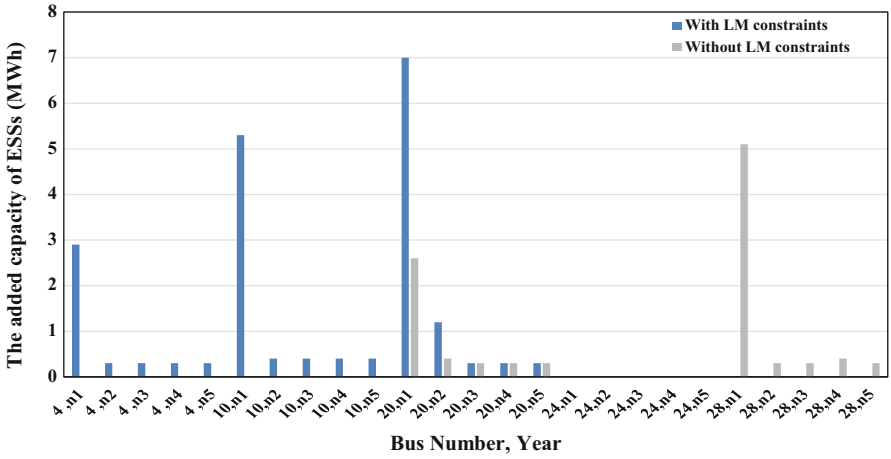

Fig. 14.8 The added capacity of ESSs in each bus number for planning horizon in, Case-II

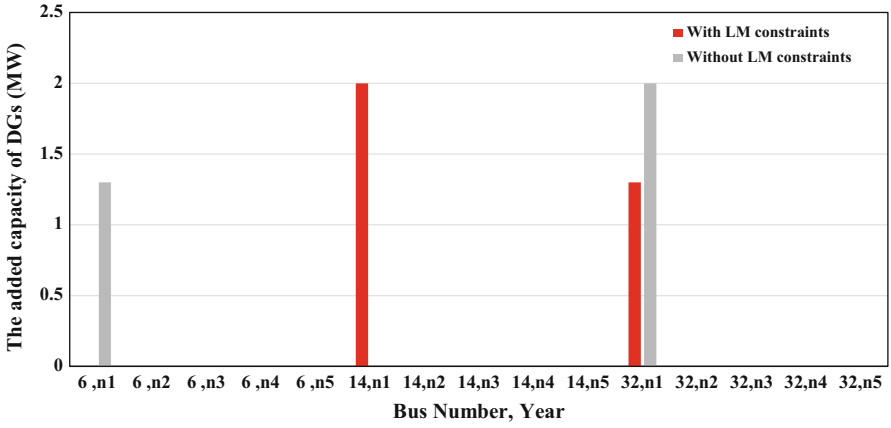

Fig. 14.9 The added capacity of DGs in each bus number for planning horizon, in Case-II

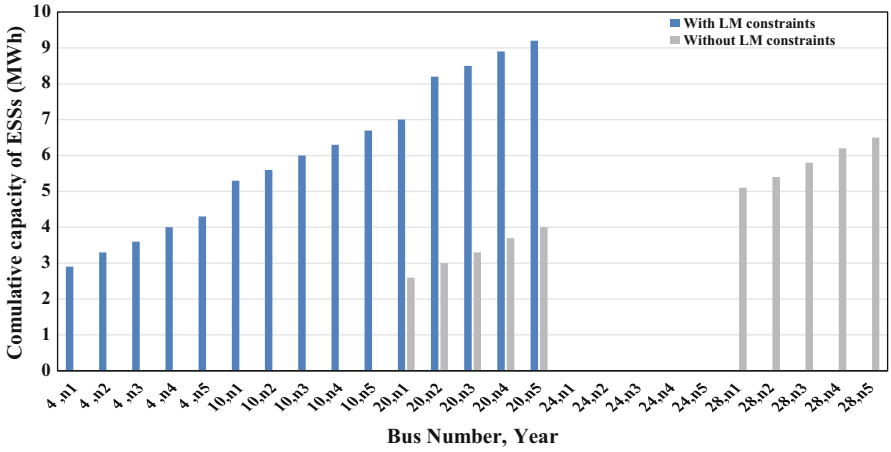

Fig. 14.10 Total capacity of ESSs in each bus number for planning horizon, in Case-II

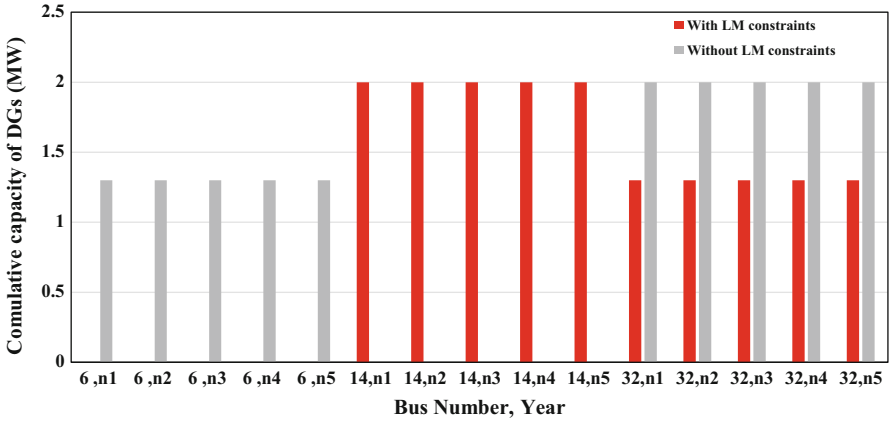

Fig. 14.11 Total capacity of DGs in each bus number for planning horizon, in Case-II

and ESSs energy to the system is affected by the voltage stability constraint. Also, more capacity is needed in order to guarantee the system security, when the voltage stability is considered in planning horizon.

Also, Figs. 14.10 and 14.11 show the total installed capacity of ESSs and DGs for this case, respectively. As it is evident from these figures total capacity of DGs and ESSs are affected by LM constraints in such a way that capacity of DGs and ESSs with the voltage stability constraints is bigger than those of without LM constraints.

Table 14.7 DG owner profit and power generation cost for all cases

Case #	DG owner profit ($)	Power generation cost ($)
Case-I	0	4103451.9
Case-II	875527.7	0
Case-III	906035.2	4260600.0

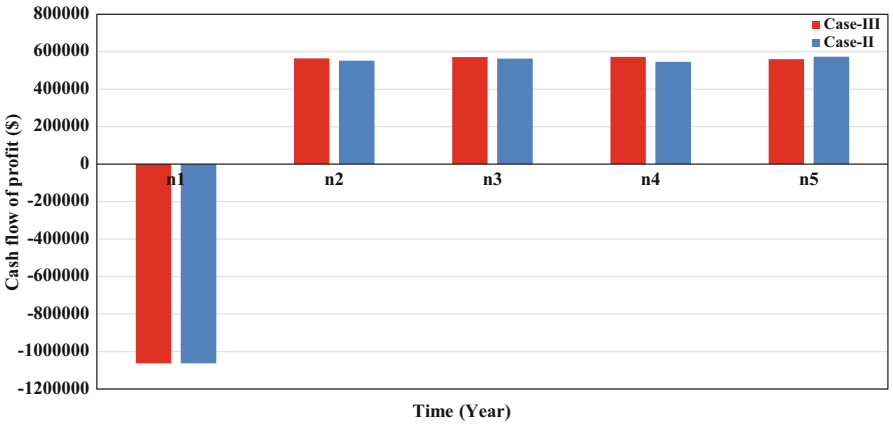

Fig. 14.12 Cash flow of DG owner's profit in different cases for the entire planning horizon

14.4.4 Case-III: From the Perspective of Both DG Owner and DSO, Simultaneously

In this case, the proposed VSC-WSPM is solved from both perspectives of DG owner and DSO. For the sake of comparison, the results obtained in this case are compared with two other cases when voltage stability constraints considered for all cases. It is assumed that desired LM is 5%. The net profit obtained from selling wind energy and power generation cost in all cases are tabulated in Table 14.7. It is evident from this table that considering both perspectives simultaneously provides more profit for the DG owner contrary to DSO. Also, Fig. 14.12 depicts the cash flow of profit obtained by DG owner in planning horizon for Case-II and Case-III. As it is observed from this figure that in the first year of planning the annual profit is negative, which means that the investment is not yet profitable in this year. Also, in the last 4 years, the profit becomes positive and is different for two cases.

The obtained annual capacity of ESSs and DGs which will be installed in the entire horizon is depicted in Figs. 14.13 and 14.14 for all cases, respectively. As it is observed in these figures, the added capacity of ESSs and DGs depends on the objective of decision maker and changes in different years due to the demand growth.

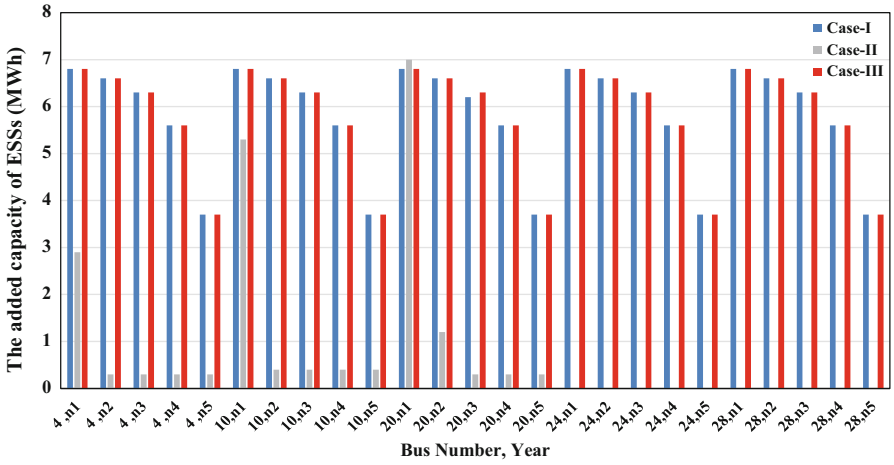

Fig. 14.13 The added capacity of ESSs in each bus number for planning horizon for different cases

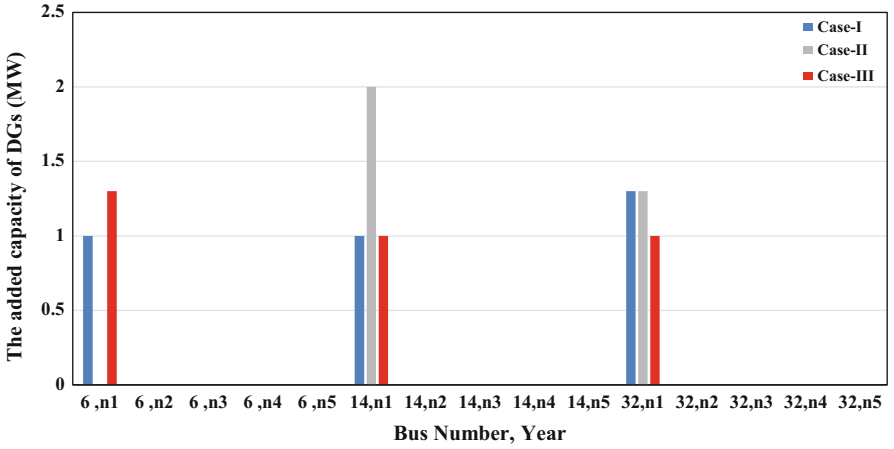

Fig. 14.14 The added capacity of DGs in each bus number for planning horizon for different cases

The cumulative capacity of ESSs and DGs in the planning horizon is given in Figs. 14.15 and 14.16 for all cases, respectively. As it is observed from these figures, the total capacities of ESSs and DGs are not the same in different cases. In other words, the capacity of DGs and ESSs depends on the goals of DG owner and DSO. Correspondingly, DSO and DG owner should specify their strategies when they make a planning decision.

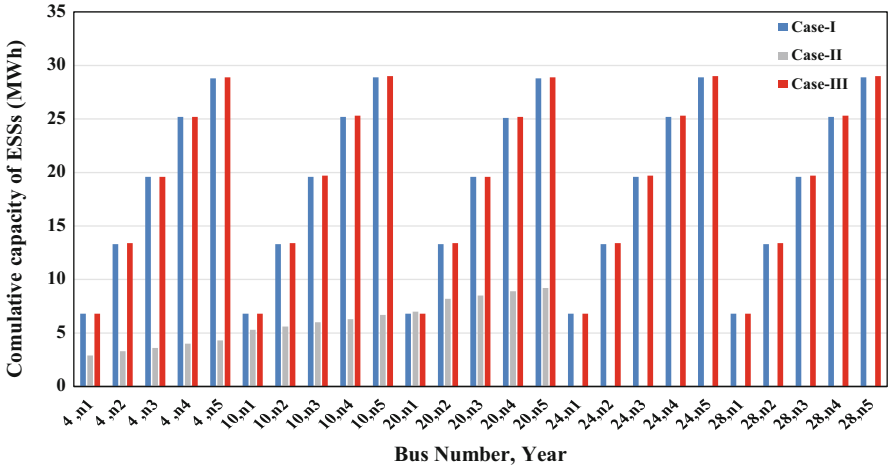

Fig. 14.15 Total capacity of ESSs in each bus number for planning horizon for different cases

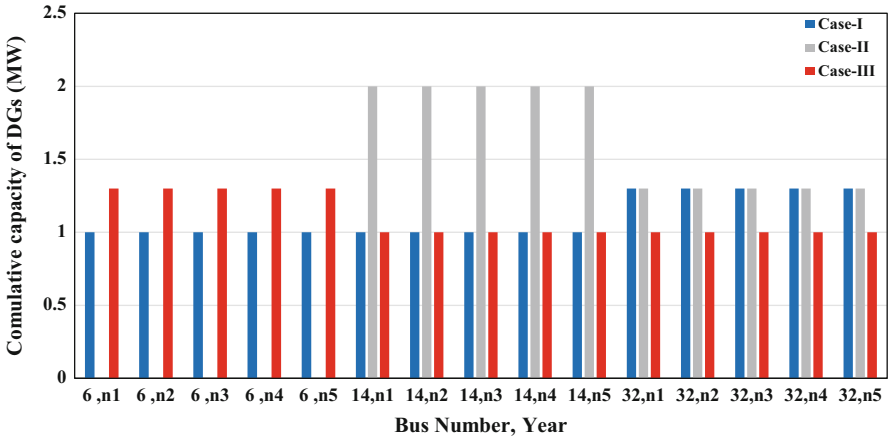

Fig. 14.16 Total capacity of DGs in each bus number for planning horizon for different cases

As it is aforementioned, one of the advantages of ESS is increasing wind power penetration. In this part, the impact of ESSs on capacity of DGs is investigated. In this regard, the proposed model is solved with and without ESS and total capacity of DGs is compared. It is evident from Fig. 14.17 that including ESSs to the grid increases the wind energy penetration in planning horizon.

Due to the relationship of SOC and ESS charge/discharge capacity, SOC can be used to investigate the charge/discharge states of ESS. The SOC of ESSs at buses 10 and 20 for third and fifth year of planning is depicted in Figs. 14.18 and 14.19,

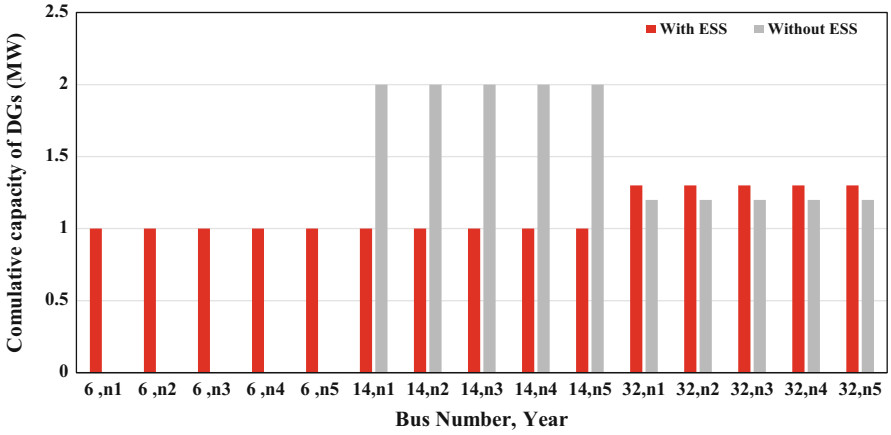

Fig. 14.17 The added capacity of DGs with and without ESS

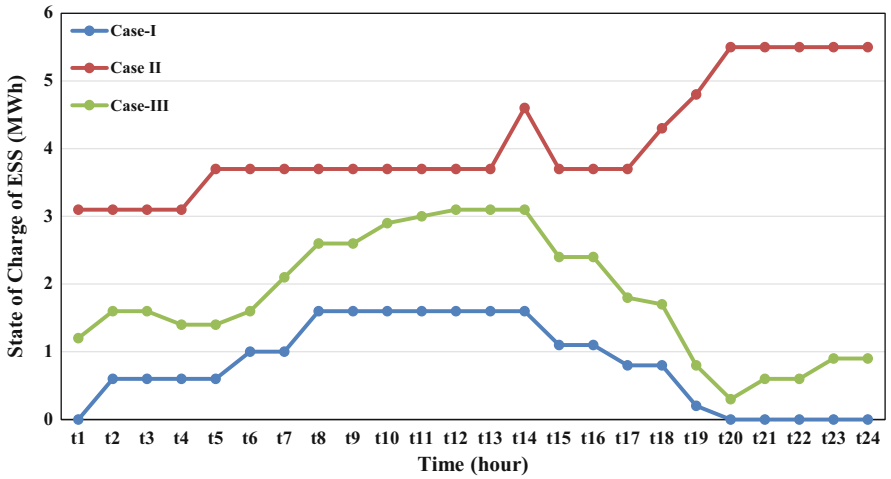

Fig. 14.18 SOC of ESS for bus 10 in third year of planning for a day in different cases

respectively. As it is observed from these figures, SOC increases and decreases in different time intervals of a day. Also, it is observed that in Case-II SOC is greater than other two cases, which is because of objective function of this case that ESS charge and discharge cost have not been considered in objective function. Furthermore, due to the topology of grid, SOC is different in ESS installed buses.

In this part, sensitivity of OF (i.e., in Eq. (14.7)) with respect to variation of interest rate in Case-III is investigated. Figure 14.20 depicts the variation of OF when the interest rate increases from 4% to 8% and inflation rate is kept 1%.

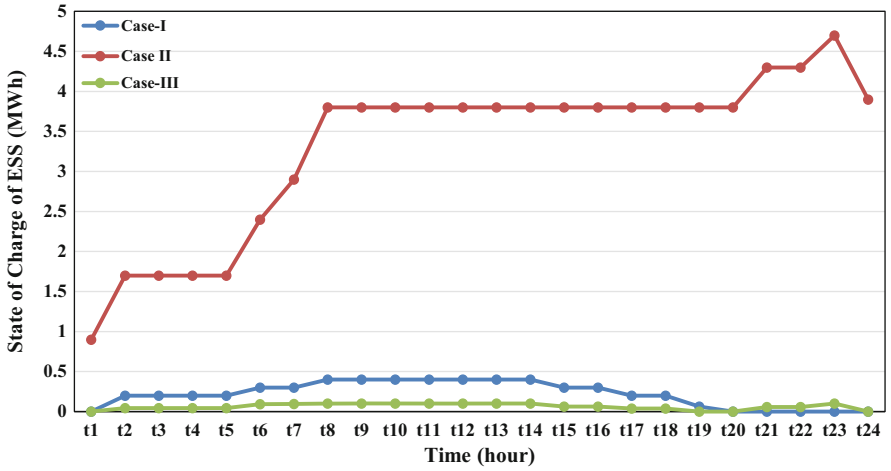

Fig. 14.19 SOC of ESS for bus 20 in fifth year of planning for a day in different cases

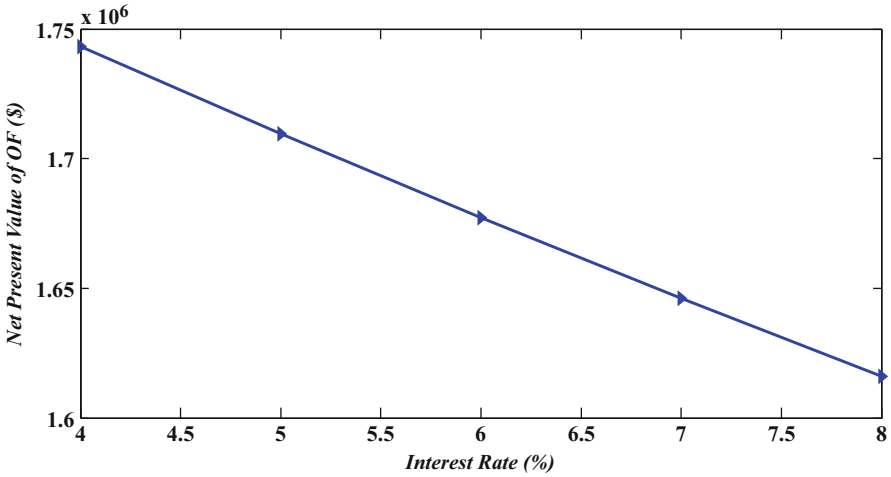

Fig. 14.20 Variation of net present value of OF versus the interest rate changes

It is inferred from this figure that if the interest rate increases, the OF reduces accordingly. Therefore the DG investor and DSO should consider proper value for the interest rate of their investments.

Finally, the P-V curve of an arbitrary load bus, i.e., bus 17 in the last year of the planning (i.e., fifth year) is depicted in Fig. 14.21. The P-V curves are plotted at the peak loading condition (i.e., t_{15}) for all three cases.

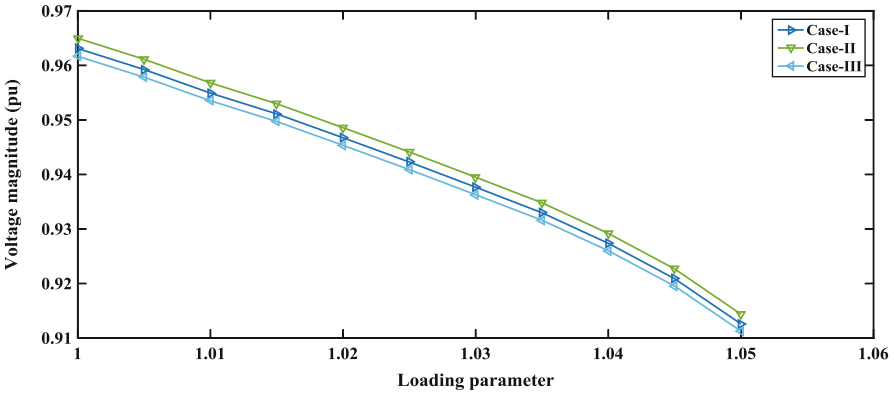

Fig. 14.21 Voltage profile of bus 17 in fifth year of planning horizon, at peak loading condition (t_{15})

14.5 Conclusion

In this chapter an approach is proposed for joint ESS and DG long-term planning, considering voltage stability constraints. Among the voltage stability indices, loading margin (LM) is considered in the formulation of the VSC-WSPM model. The proposed VSC- WSPM approach offers a decision-making tool for both DSO and DG owner to optimally determine their own strategies for utilization of wind energy and ESS.

The proposed VSC-WSPM is implemented on the IEEE 33-bus distribution test system in different cases. In the first case, the problem is solved from the perspective of DSO with the aim of power generation and ESS charge/discharge costs minimization, and the effect of voltage stability constraints on capacity of DGs and ESSs is investigated. In the second case, the problem is solved from the perspective of DG owner with the objective of maximizing his/her profit from wind energy procurement. In this case the capacity of ESSs and DGs is determined, with and without voltage stability constraints. In the third case, the problem solved from the perspective of both DSO and DG owner and the results compared with the former two cases when voltage stability constraints are taken into consideration. The following conclusions can be drawn:

- At the presence of voltage stability constraints the scheduled capacity of DGs and ESSs increases in order to preserve the voltage stability by ensuring the desired value of LM.
- It is necessary to charge the ESSs when DG owner wants to inject more wind energy to the grid. In such case, the SOC of ESSs is higher than the other cases.
- The added capacity of wind energy and ESS depends on the aims and priorities of the decision makers.

- The scheduled capacity of ESSs and DGs is affected by voltage stability constraints.
- DG owner and DSO should consider proper interest rate for their long-term investments.

Nomenclature

Sets

N_B	System buses
N_G	Generating units
N_L	Transmission lines
N_T	Planning horizon
N_{DG}	DG installed buses
N_{ESS}	ESS installed buses

Indices

b	System buses index
DG	DGs index
ESS	ESSs index
i	Thermal generating units' index
l	Transmission lines index
n	Index of planning years
t	Time index

Variables and Parameters

ϑ	Inflation rate
ε	Interest rate
ρ	Wind energy penetration factor
λ	Loading parameter
$\beta_{b,\,n}$	Demand growth rate at bus b in year n.
λ_{des}	Desired LM
$\eta_{b,t}^{\mathrm{ch/disch}}$	Efficiency of charging and discharging of ESS (%)

$\delta_{b,t}^{\text{ch/disch}}$	Charge/discharge binary indicators of ESSs
Δt	Timeslot duration
$\pi_{b,n}^{\text{DG}}$	Cumulative wind power capacity of DG connected to bus b up to year n
$\text{CHC}_{n,\,t}$.	Charge/discharge cost in year n and time t (\$/MWh)
CF_t^{DG}	Capacity factor of DG in time t
DGC_{inv}	Investment cost of DGs (\$/MW)
$\text{DGC}_{\text{O \& M}}$	Operation and maintenance cost of DGs (\$/MWh)
$E_{b,n}^{\text{ESS}}$	Actual capacity of the ESS connected to bus b, in year n
$e_{b,n}^{\text{ESS}}$	Added ESS capacity to bus b, in year n
$e_{\max}^{\text{ESS}}$	Maximum annual added ESS capacity to the grid
$\text{EC}_{n,\,t}$.	Energy price in year n and time t (\$/MWh)
$I_{b,n}^{\text{DG}}$	Binary indicators of DGs
$K_{G,\,i}$	Rate of change in active power generation of unit i
$K_{D,\,b}$	Rate of load change at bus b
$P_{b,n}^{\text{DG}}$	The added wind power capacity for DG connected to bus b in year n
$P_{\max\,/\,\min}^{\text{DG}}$	Maximum/minimum wind energy added to the grid
$p_{b,n,t}^{\text{CH/DISCH}}$	Charge/discharge power of ESS at node b in year n, at time t
$p_{b,t}^{\text{ch/disch,max}}$	Maximum power charge/discharge of ESS at node b and time t
$(P/Q)_{G_i}^{\max\,/\,\min}$	Maximum/minimum active/reactive power of ith thermal generation unit
$P_{i,n,t}^{G}/Q_{i,n,t}^{G}$	Active/reactive power generation by ith thermal generation unit in year n, at time t
$\widehat{P}_{i,n,t}^{G}/\widehat{Q}_{i,n,t}^{G}$	Active/reactive power production of generator i in year n and time t at LLP
$P_{b,n,t}^{D}/Q_{b,n,t}^{D}$	Active/reactive power load of bus b in year n, at time t
$\widehat{P}_{b,t,d}^{D}/\widehat{Q}_{b,t,d}^{D}$	Active/reactive power consumption of load connected to bus b in year n and time t at LLP
$p_{b,n,t}^{\text{DG}}/q_{b,n,t}^{\text{DG}}$	Active/reactive power of DG injected to bus b in year n, at time t
$q_{b,\max\,/\,\min}^{\text{DG}}$	Maximum/minimum reactive power of DG injected to bus b
$S_{l,\,n,\,t}(V,\theta)$	Power flow through l-th transmission line in year n, at time t
$S_l^{\max}$	Maximum transferable power through line l
$\text{SOC}_{b,n,t}^{\text{ESS}}$	State of charge (SOC) for the ESS connected at bus b in year n, at time t
$\text{SOC}_b^{\max\,/\,\min}$	Maximum/minimum value of SOC
$V_{b,\,n,\,t}/\theta_{b,\,n,\,t}$	Voltage magnitude/angle of bus b in year n, at time t
$\widehat{V}_{b,t,d}/\widehat{\theta}_{b,t,d}$	Voltage magnitude/angle of bus b in year n and time t at LLP
$V_b^{\max\,/\,\min}$	Maximum/minimum voltage in bus b
Y_{bj}/ϕ_{bj}	Magnitude/angle of bj-th element of system admittance matrix

References

1. Gyuk IP, Eckroad S (2004) Energy storage for grid connected wind generation applications, US Department of Energy, Washington DC, EPRI-DOE Handbook Supplement, vol 1008703
2. Chen C, Duan S, Cai T, Liu B, Hu G (2011) Optimal allocation and economic analysis of energy storage system in microgrids. IEEE Trans Power Electron 26(10):2762–2773. https://doi.org/10.1109/TPEL.2011.2116808
3. Barton JP, Infield DG (2004) Energy storage and its use with intermittent renewable energy. IEEE Trans Energy Convers 19(2):441–448. https://doi.org/10.1109/TEC.2003.822305
4. Zhang Y, Dong ZY, Luo F, Zheng Y, Meng K, Wong KP (2016) Optimal allocation of battery energy storage systems in distribution networks with high wind power penetration. IET Renew Power Gener 10(8):1105–1113. https://doi.org/10.1049/iet-rpg.2015.0542
5. Atwa YM, El-Saadany E (2010) Optimal allocation of ESS in distribution systems with a high penetration of wind energy. IEEE Trans Power Syst 25(4):1815–1822. https://doi.org/10.1109/TPWRS.2010.2045663
6. Xiong P, Singh C (2016) Optimal planning of storage in power systems integrated with wind power generation. IEEE Trans Sustainable Energy 7(1):232–240. https://doi.org/10.1109/TSTE.2015.2482939
7. Maghouli P, Soroudi A, Keane A (2016) Robust computational framework for mid-term techno-economical assessment of energy storage. IET Gener Transm Distrib 10(3):822–831. https://doi.org/10.1049/iet-gtd.2015.0453
8. Farzin H, Fotuhi-Firuzabad M, Moeini-Aghtaie M (2017) A stochastic multi-objective framework for optimal scheduling of energy storage systems in microgrids. IEEE Trans Smart Grid 8(1):117–127. https://doi.org/10.1109/TSG.2016.2598678
9. Jabr RA, Džafić I, Pal BC (2015) Robust optimization of storage investment on transmission networks. IEEE Trans Power Syst 30(1):531–539. https://doi.org/10.1109/TPWRS.2014.2326557
10. Soroudi A, Siano P, Keane A (2016) Optimal DR and ESS scheduling for distribution losses payments minimization under electricity price uncertainty. IEEE Trans Smart Grid 7(1):261–272. https://doi.org/10.1109/TSG.2015.2453017
11. Le HT, Santoso S, Nguyen TQ (2012) Augmenting wind power penetration and grid voltage stability limits using ESS: application design, sizing, and a case study. IEEE Trans Power Syst 27(1):161–171. https://doi.org/10.1109/TPWRS.2011.2165302
12. Malysz P, Sirouspour S, Emadi A (2014) An optimal energy storage control strategy for grid-connected microgrids. IEEE Trans Smart Grid 5(4):1785–1796. https://doi.org/10.1109/TSG.2014.2302396
13. Murillo-Sanchez CE, Zimmerman RD, Anderson CL, Thomas RJ (2013) Secure planning and operations of systems with stochastic sources, energy storage, and active demand. IEEE Trans Smart Grid 4(4):2220–2229. https://doi.org/10.1109/TSG.2013.2281001
14. Chen H, Zhang R, Li G, Bai L, Li F (2016) Economic dispatch of wind integrated power systems with energy storage considering composite operating costs. IET Gener Transm Distrib 10(5):1294–1303. https://doi.org/10.1049/iet-gtd.2015.0410
15. Luo F, Meng K, Dong ZY, Zheng Y, Chen Y, Wong KP (2015) Coordinated operational planning for wind farm with battery energy storage system. IEEE Trans Sustainable Energy 6(1):253–262. https://doi.org/10.1109/TSTE.2014.2367550
16. Ghofrani M, Arabali A, Etezadi-Amoli M, Fadali MS (2013) A framework for optimal placement of energy storage units within a power system with high wind penetration. IEEE Trans Sustainable Energy 4(2):434–442. https://doi.org/10.1109/TSTE.2012.2227343
17. Chacra FA, Bastard P, Fleury G, Clavreul R (2005) Impact of energy storage costs on economical performance in a distribution substation. IEEE Trans Power Syst 20(2):684–691. https://doi.org/10.1109/TPWRS.2005.846091

18. Abbey C, Joós G (2009) A stochastic optimization approach to rating of energy storage systems in wind-diesel isolated grids. IEEE Trans Power Syst 24(1):418–426. https://doi.org/10.1109/TPWRS.2008.2004840
19. Rabiee A, Soroudi A, Mohammadi-Ivatloo B, Parniani M (2014) Corrective voltage control scheme considering demand response and stochastic wind power. IEEE Trans Power Syst 29(6):2965–2973. https://doi.org/10.1109/TPWRS.2014.2316018
20. Rabiee A, Nikkhah S, Soroudi A, Hooshmand E (2016) Information gap decision theory for voltage stability constrained OPF considering the uncertainty of multiple wind farms. IET Renew Power Gener 11(5):585–592. https://doi.org/10.1049/iet-rpg.2016.0509
21. Mohseni-Bonab SM, Rabiee A, Mohammadi-Ivatloo B (2016) Voltage stability constrained multi-objective optimal reactive power dispatch under load and wind power uncertainties: a stochastic approach. Renew Energy 85:598–609. https://doi.org/10.1016/j.renene.2015.07.021
22. Hung DQ, Mithulananthan N, Bansal R (2014) Integration of PV and BES units in commercial distribution systems considering energy loss and voltage stability. Appl Energy 113:1162–1170. https://doi.org/10.1016/j.apenergy.2013.08.069
23. Sugihara H, Yokoyama K, Saeki O, Tsuji K, Funaki T (2013) Economic and efficient voltage management using customer-owned energy storage systems in a distribution network with high penetration of photovoltaic systems. IEEE Trans Power Syst 28(1):102–111. https://doi.org/10.1109/TPWRS.2012.2196529
24. Lee SJ, Kim JH, Kim CH, Kim SK, Kim ES, Kim DU, Mehmood KK, Khan SU (2016) Coordinated control algorithm for distributed battery energy storage systems for mitigating voltage and frequency deviations. IEEE Trans Smart Grid 7(3):1713–1722. https://doi.org/10.1109/TSG.2015.2429919
25. Arulampalam A, Barnes M, Jenkins N, Ekanayake JB (2006) Power quality and stability improvement of a wind farm using STATCOM supported with hybrid battery energy storage. IEE Proc-Gener Transm Distrib 153(6):701–710. https://doi.org/10.1049/ip-gtd:20045269
26. Le HT, Santoso S (2007) Analysis of voltage stability and optimal wind power penetration limits for a non-radial network with an energy storage system. In: IEEE General Meeting in Power Engineering Society, IEEE, pp 1–8. https://doi.org/10.1109/PES.2007.385735
27. Rabiee A, Soroudi A, Keane A (2015) Information gap decision theory based OPF with HVDC connected wind farms. IEEE Trans Power Syst 30(6):3396–3406. https://doi.org/10.1109/TPWRS.2014.2377201
28. Rabiee A, Parniani M (2013) Voltage security constrained multi-period optimal reactive power flow using benders and optimality condition decompositions. IEEE Trans Power Syst 28(2):696–708. https://doi.org/10.1109/TPWRS.2012.2211085
29. Rabiee A, Soroudi A, Keane A (2015) Risk-averse preventive voltage control of ac/dc power systems including wind power generation. IEEE Trans Sustainable Energy 6(4):1494–1505. https://doi.org/10.1109/TSTE.2015.2451511
30. Brooke A, Kendrick D, Meeraus A, Raman R, Rosenthal R (1998) GAMS: a user's guide. GAMS Development Corporation, Washington, DC
31. Brooke A, Kendrick D, Meeraus A, Raman R, Rosenthal R (1998) GAMS: the solver manuals. GAMS Development Corporation, Washington, DC
32. Bussieck MR, Vigerske S (2010) MINLP solver software. In: Wiley encyclopedia of operations research and management science. Wiley, Hoboken. https://doi.org/10.1002/9780470400531.eorms0527
33. Ameli A, Bahrami S, Khazaeli F, Haghifam MR (2014) A multiobjective particle swarm optimization for sizing and placement of DGs from DG owner's and distribution company's viewpoints. IEEE Trans Power Delivery 29(4):1831–1840. https://doi.org/10.1109/TPWRD.2014.2300845